Model referencyjny w odpornym na uszkodzenia napędzie z silnikiem reluktancyjnym przełączalnym

Bogdan Fabiański

Politechnika Poznańska
Instytut Automatyki i Inżynierii Informatycznej

10.06.2016

PLAN WYSTĄPIENIA

- Silnik SRM
- Model matematyczny
- Adaptacja parametrów modelu
- Początkowy kąt obrotu wału
- Kształtowanie prądu silnika
- Optymalizacja kątów wysterowania
- Blok detekcji uszkodzeń
- Podsumowanie

Silnik SRM

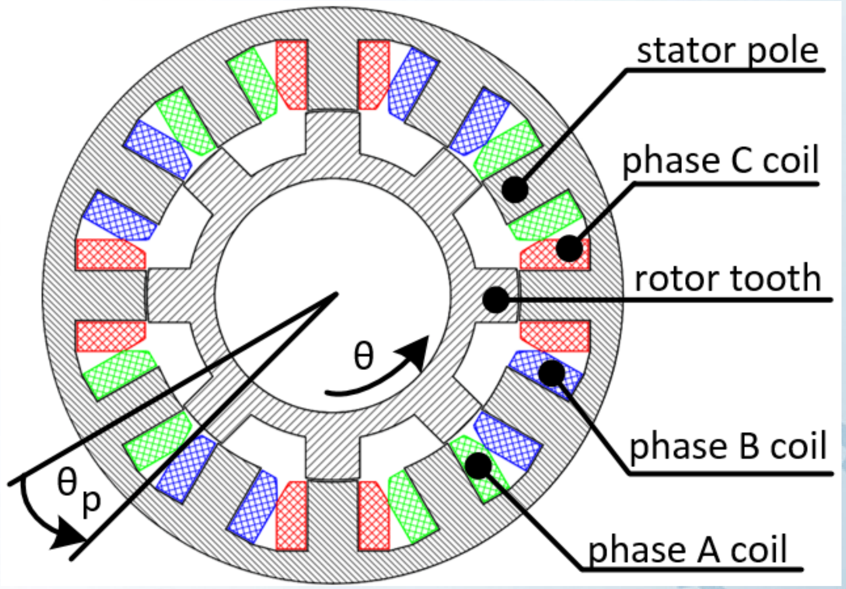

Rysunek 1: Cross-section schema of the 3-phase SRM that bases on 12/8 poles structure

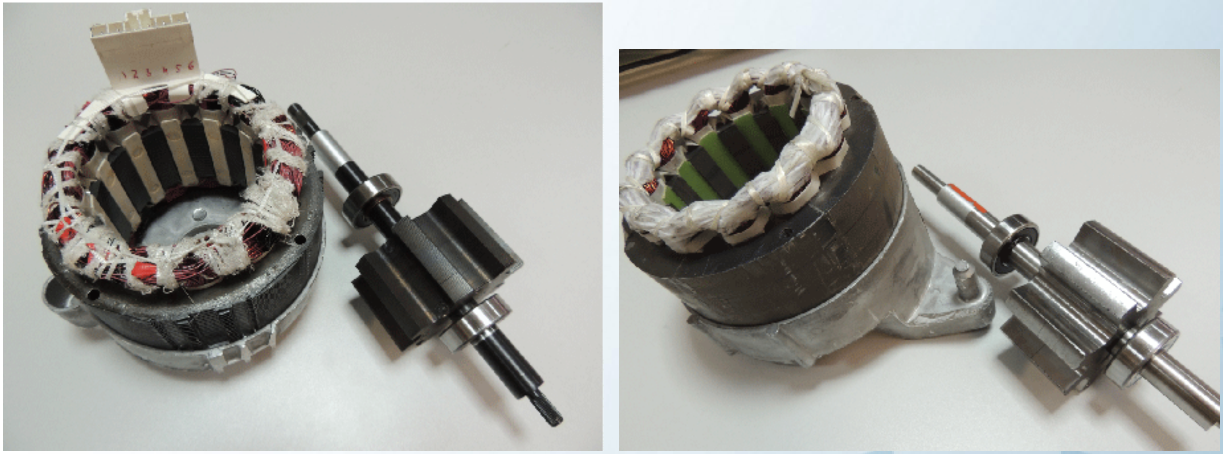

Rysunek 2: Examples of the 12/8 poles motors

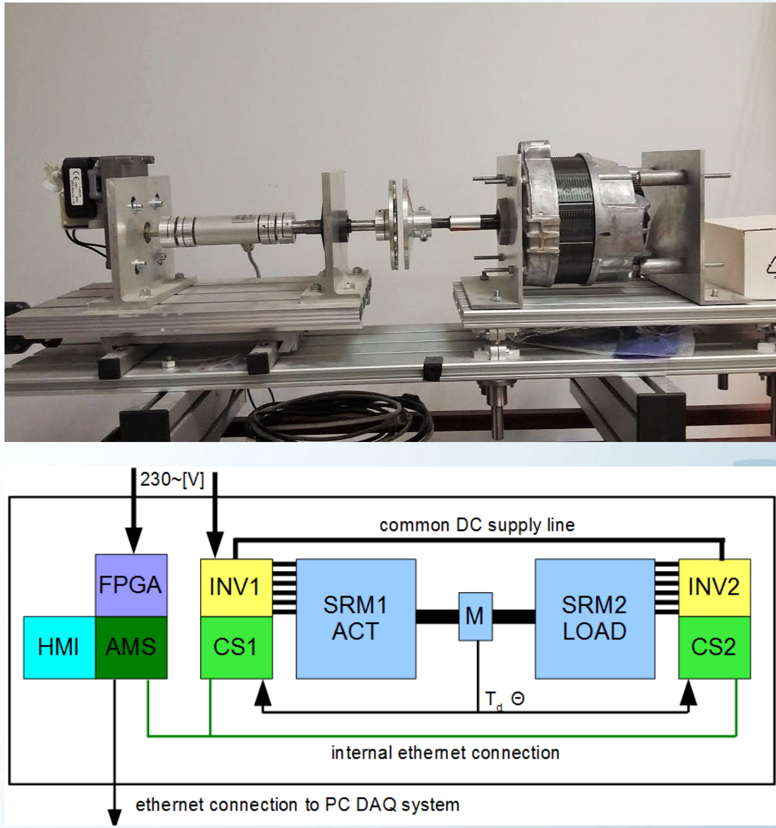

Rysunek 3: Experimental stand

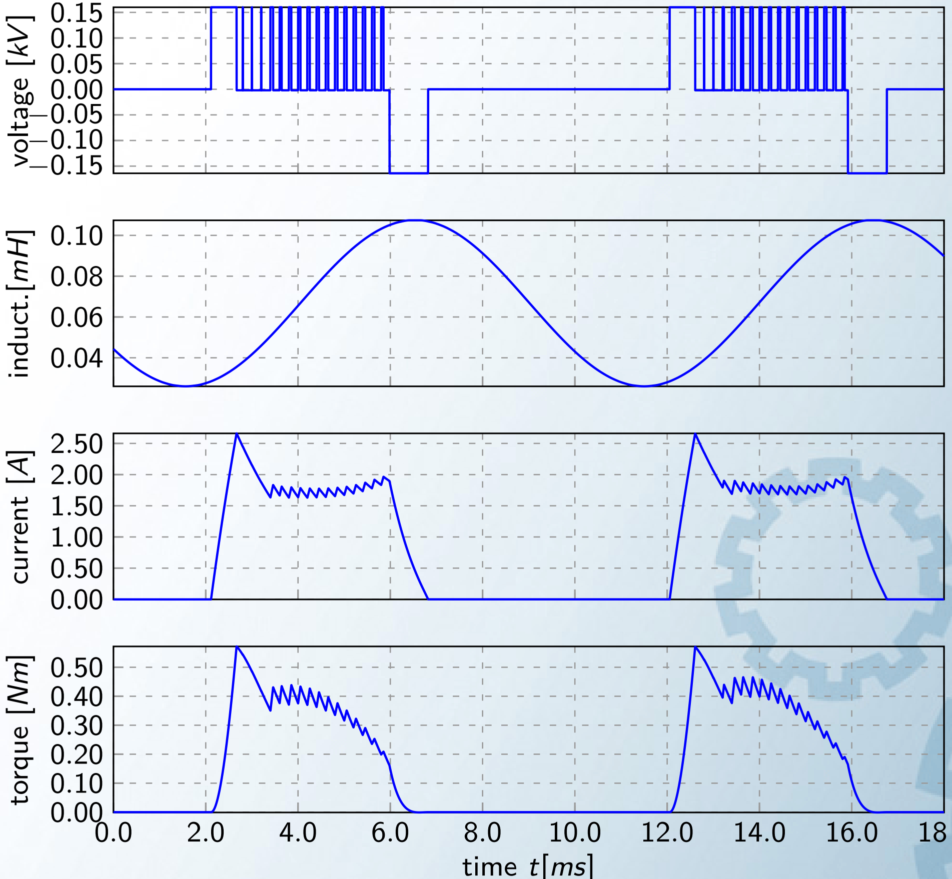

voltage [kV]
0.15
0.10
0.05
0.00
−0.05
−0.10
−0.15
induct.[mH]
0.10
0.08
0.06
0.04
current [A]
2.50
2.00
1.50
1.00
0.50
0.00
torque [Nm]
0.50
0.40
0.30
0.20
0.10
0.00
0.0
2.0
4.0
6.0
8.0
10.0
12.0
14.0
16.0
18
time t[ms]

The figure 6 shows how the torque generated by all phases independently (top of the figure) affects the overall motor value (bottom, as the result of phases generation sum).

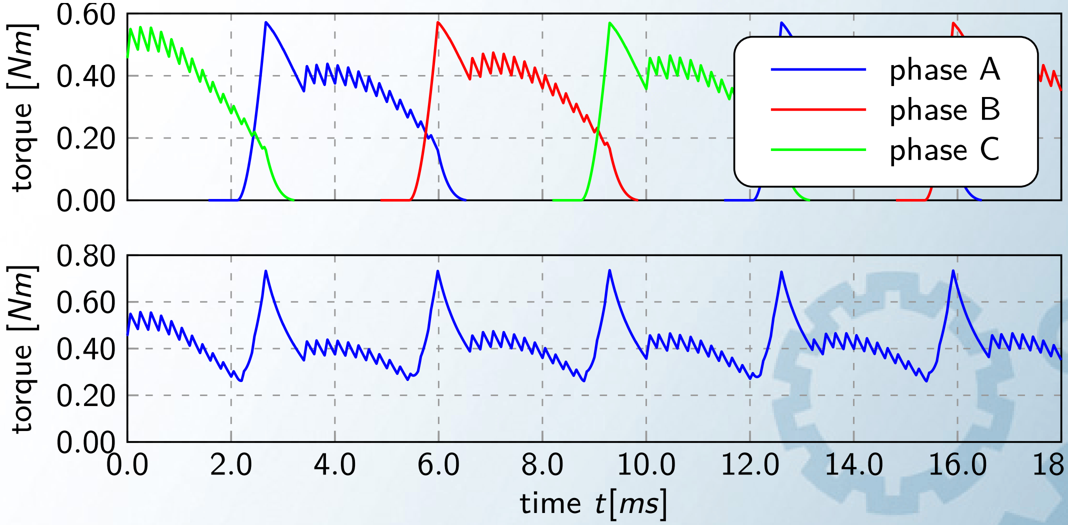

Rysunek 5: Torque value generated by all phases independently (top) and overall torque value (bottom)

The figure 6 shows how the torque generated by all phases independently (top of the figure) affects the overall motor value (bottom, as the result of phases generation sum).

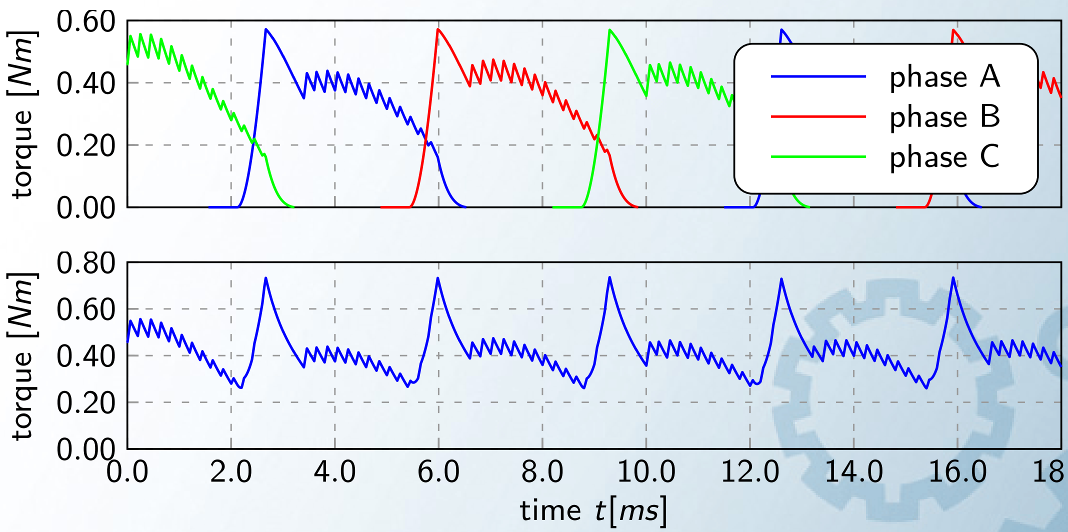

Rysunek 6: Torque value generated by all phases independently (top) and overall torque value (bottom)

Model matematyczny

Równania podstawowe - model liniowy

$$v_p = i_p R_p + v_{pF}, \tag{1}$$

where: $i_p(A)$ – phase winding current, $R_p(\Omega)$ – phase winding resistance, $v_{pF}(V)$ – voltage sourced in Faraday's induction law,

$$v_{pF} = \frac{d\Psi_p}{dt}, \tag{2}$$

$\Psi_p(Wb)$ – phase winding magnetic flux linkage, $t(s)$ – time. In general case, where the flux linkage is a function of two variables: θ_p – motor rotor angle and i_p – phase current, equation (2) can be expanded to the form:

$$v_{pF} = \frac{d\Psi_p(i_p, \theta_p)}{dt}, \tag{3}$$

$$v_{pF} = \frac{\partial \Psi_p(i_p, \theta_p)}{\partial i_p}\frac{di_p}{dt} + \frac{\partial \Psi(i_p, \theta_p)}{\partial \theta_p}\frac{d\theta_p}{dt}. \tag{4}$$

$$\Psi_p(\theta_p) = L_p(\theta_p) i_p, \tag{5}$$

where: $L_p(H)$ – phase winding inductance. Equation (5) applied to (1) and (4) gives:

$$v_p = i_p R_p + L_p(\theta_p)\frac{di_p}{dt} + \frac{dL_p(\theta_p)}{d\theta_p} i_p \omega, \tag{6}$$

from where can be seen that expression:

$$\epsilon_p = \frac{dL_p(\theta_p)}{d\theta_p} i_p \omega \tag{7}$$

is an electromotive force (ϵ_p) generated in motor winding dependent from rotor speed $\omega = \frac{d\theta_p}{dt}$.

Mechanical power P_{me} consumed to generate electromagnetic torque T_p can be expressed as an difference between supplied electrical power P_{el} and power of the phase coil magnetic field plus resistive loses ($P_R = {i_p}^2 R_p$):

$$P_{me} = P_{el} - (P_{ma} + P_R). \tag{8}$$

If consider P_{el} from product of equation (6) and phase current (i_p), there is:

$$P_{me} = T_p \omega = T_p \frac{d\theta_p}{dt}, \tag{9}$$

and power of magnetic field P_{ma}:

$$P_{ma} = \frac{\int_{i_p} L(\theta_p) i_p di}{dt}, \tag{10}$$

$$P_{ma} = L_p(\theta_p) i_p \frac{di_p}{dt} + \frac{1}{2} i^2 \omega \frac{dL_p(\theta_p)}{d\theta_p}. \tag{11}$$

Equations (8),(9),(11) gives finally:

$$T_p = \frac{1}{2} i^2 \frac{dL_p(\theta_p)}{d\theta_p}. \tag{12}$$

Model nieliniowy

Unfortunately, model based on formulas (6) and (12) provides a good agreement with experimental results only in the range of small currents. To make more accurate model, the equation (5) could be written in the form:

$$\Psi_p(\theta_p) = L_p(\theta_p) sat(i_p), \tag{13}$$

where: $sat(i_p)$ – saturation function of the phase current (i_p). The role of the $sat(i_p)$ from equation (13) is to take account of the saturation of the magnetic circuit. When (11) applied to the phase voltage equation (1) and (4) it can be written:

$$v_p = i_p R_p + \frac{d\Psi_p(i_p, \theta_p)}{dt}. \tag{14}$$

If assumed v,i,R,L related to the motor phase winding (subscript p), expression (14) may be expanded to the form:

$$v = iR + \frac{\partial(L(\theta) sat(i))}{\partial i}\frac{di}{dt} + \frac{\partial(L(\theta) sat(i))}{\partial \theta}\frac{d\theta}{dt}. \tag{15}$$

Introducing operator D as follows:

$$D(F(x)) = \frac{\partial F(x)}{\partial x} \tag{16}$$

equation (15) can be write in the form:

$$v = iR + L(\theta)D(sat(i))\frac{di}{dt} + D(L(\theta))sat(i)\omega, \tag{17}$$

where: D – differential operator of the dependent variable indicated in parentheses. There can be easily derived from (17) phase winding current i_p state equation:

$$\frac{di_p}{dt} = \frac{u_p - i_p R_p - D(L_p(\theta_p))sat(i_p)\omega}{L_p(\theta_p)D(sat(i_p))}. \tag{18}$$

$$P_{me} = \frac{dE_c}{dt}, \tag{19}$$

Alignment of (9) and (19) results in:

$$T_p = \frac{dE_c}{d\theta_p}. \tag{20}$$

The E_C as a current integral of flux linkage from definition gives:

$$dE_C(\theta_p, i_p) = \int_{\tau=0}^{i_p} \Psi_p(\theta_p, \tau) d\tau, \tag{21}$$

$$dE_C(\theta_p, i_p) = \int_{\tau=0}^{i_p} (L_p(\theta_p) sat(\tau)) d\tau, \tag{22}$$

$$T_p(\theta_p, i_p) = \frac{L_p(\theta_p)}{d\theta_p} \int_{\tau=0}^{i_p} (sat(\tau)) d\tau. \tag{23}$$

Introducing integral operator S of the dependent variable indicated in parentheses:

$$S(F(x)) = \int_{\tau=0}^{x} (F(\tau))d\tau, \tag{24}$$

in above equation, one can obtain:

$$T_p(\theta_p, i_p) = D(L_p(\theta_p))S(sat(i_p)), \tag{25}$$

where: S – integral operator of the dependent variable indicated in parentheses. Easily can be proved that above equation with additional form:

$$satT(i_p) = \sqrt{2S(sat(i_p))}, \tag{26}$$

gives the electromagnetic torque formula $T_p(\theta_p, i_p)$ more similar to the linear model:

$$T_p(\theta_p, i_p) = \frac{1}{2}D(L_p(\theta_p))satT(i_p)^2. \tag{27}$$

As mentioned before, overall electromagnetic torque T_e generated by motor is the sum of all torques generated by phases separately:

$$T_e(\theta_r, i_p) = \sum_{p=1}^{3} T_p(\theta_p, i_p), \tag{28}$$

where: θ_r – an absolute rotor position in relation to θ_p as follows:

$$\theta_p = \theta_r - \pi(p-1)/12. \tag{29}$$

Funkcje aproksymujące

$$\sum_{i=1}^{n}[F(x_i, p_1, ...p_k) - y_i]^2 = min, \tag{30}$$

where: n – number of sample points; i – sample point number; $F()$ – approximating function; x_i – function argument; p_l – function parameter l-numbered; y_i – measured value at i-sample; and exponential approximation function in the form:

$$F_i(x_i, \gamma, \epsilon) = \gamma(1 - e^{\epsilon x_i}), \tag{31}$$

where parameters are: γ, ϵ, and may be computed from equations:

$$\epsilon = \frac{n\sum_{i=1}^{n}(x_i ln(y_i)) - \sum_{i}^{n}(x_i)\sum_{i}^{n}(ln(y_i))}{n\sum_{i=1}^{n}x_i^2 - (\sum_{i=1}^{n}x_i)^2}, \tag{32}$$

$$\gamma = exp(\frac{\sum_{i=1}^{n}(ln(y_i)) - B\sum_{i=1}^{n}(x_i)}{n}). \tag{33}$$

For cosine approximation function:

$$F_i(x_i, \alpha) = \alpha[cos(8x_i) + 1], \tag{34}$$

parameter α can be computed from:

$$\alpha = \frac{\sum_i y_i cos(8x_i)}{\sum_i cos^2(8x_i)}. \tag{35}$$

The equation (34) as an $L_D(\theta_p)$ – dynamic inductance approximation (omitted constant minimal phase inductance – β) plus equation (35) related to the motor phase winding inductance $L_p(\theta_p)$ gives:

$$L_p(\theta_p) = L_D(\theta_p) + \beta = \alpha[cos(8\theta_p) + 1] + \beta, \tag{36}$$

where: $\theta_p \in (-\frac{\pi}{8}; \frac{\pi}{8})(rad)$; $\alpha(H)$ – dynamic inductance L_D amplitude; $\beta(H)$ – minimal measured phase inductance;

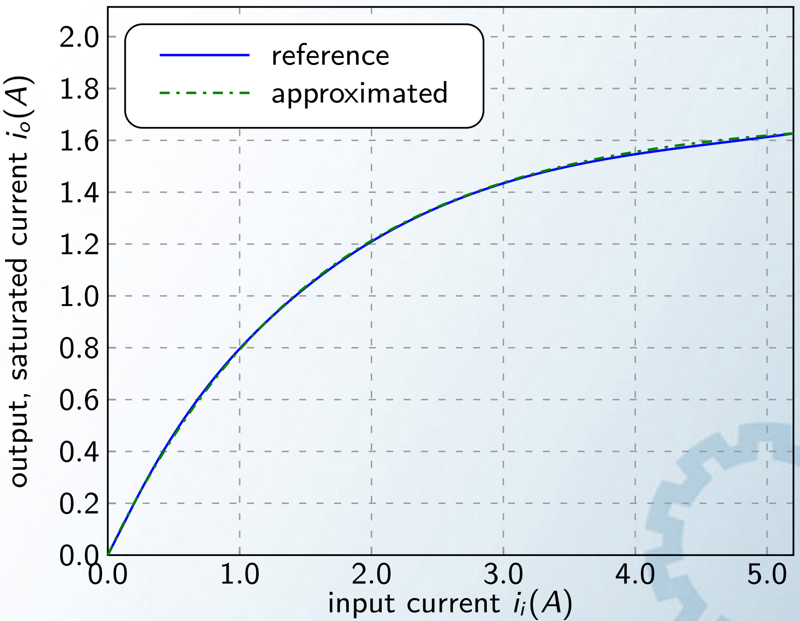

Rysunek 7: Approximation results of the $sat(i_p)$ expression to the exponential function

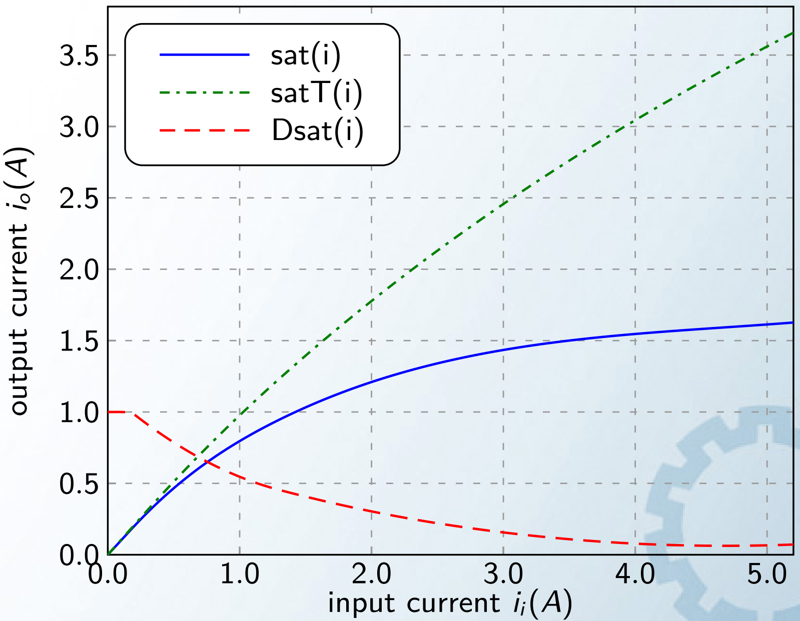

Rysunek 8: Function $sat(i)$ and its derivatives: $Dsat(i)$, $satT(i)$ plots

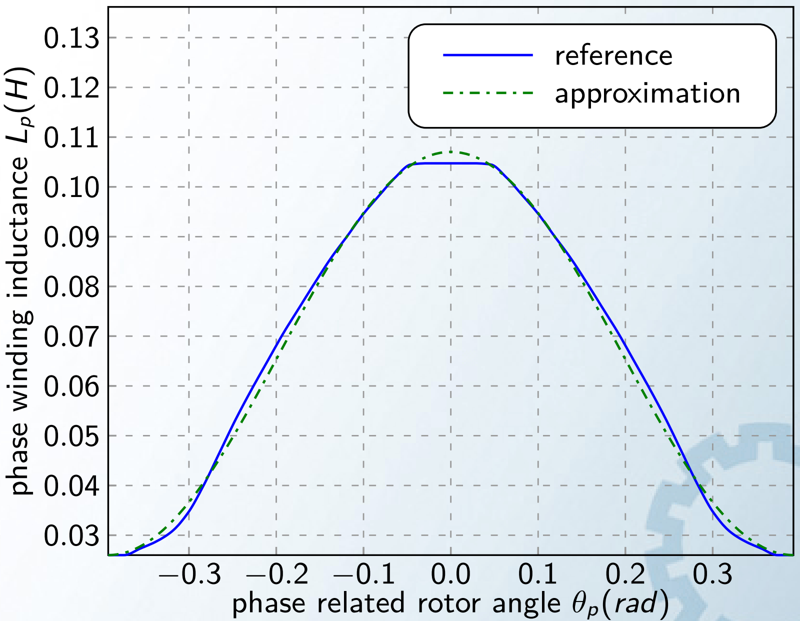

Rysunek 9: Phase inductance $L_p(\theta_p)$ plot taken from direct measure compared with its approximation to the *cos* function

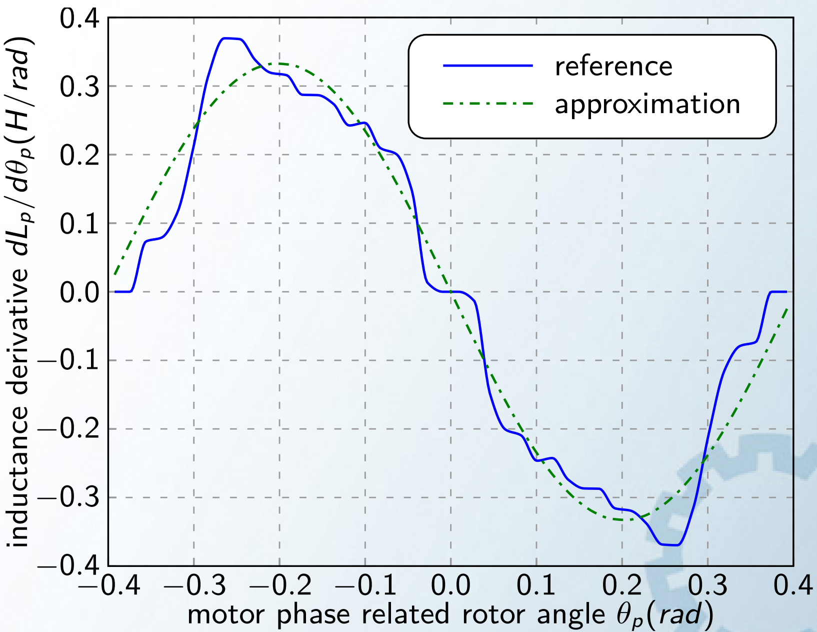

Rysunek 10: Derivatives of the phase inductance $D(L_p(\theta_p))$ from measure and of the *cos* approximation

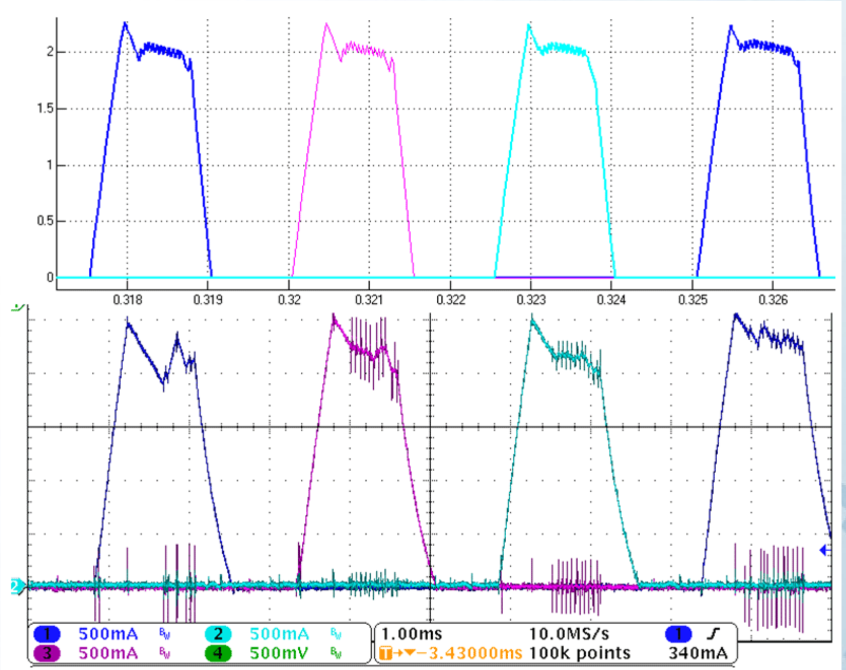

Rysunek 11: Phase currents waveforms comparison: simulation (top) and experiment (bottom) results at speed 1000 rpm, load torque 0,15 Nm; X(time) scale: 1 ms/DIV; Y(value) scale: 500 mA/DIV

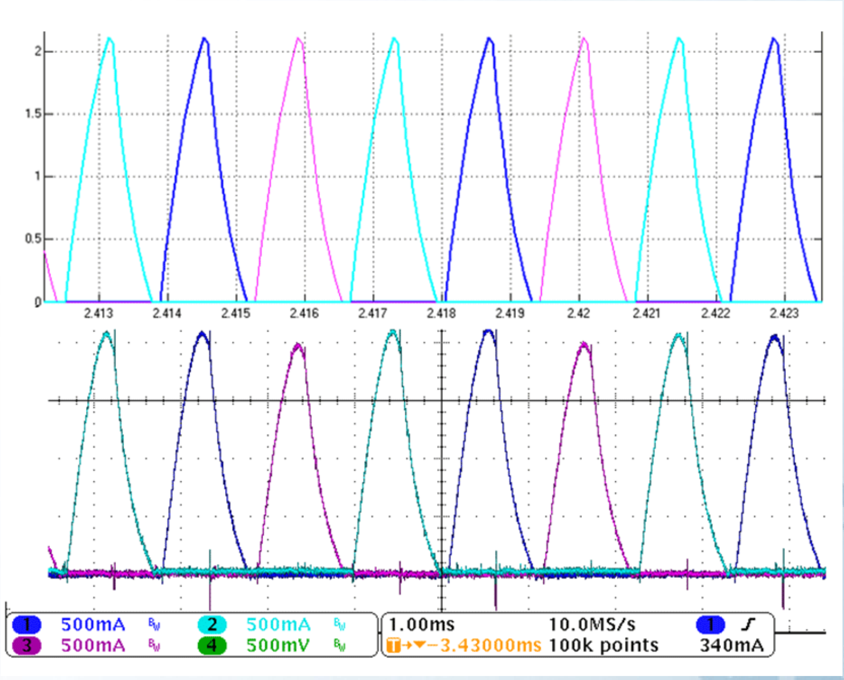

Rysunek 12: Phase currents waveforms comparison: simulation (top) and experiment (bottom) results at speed 2500 rpm, load torque 0,17 Nm; X(time) scale: 1 ms/DIV; Y(value) scale: 500 mA/DIV

Adaptacja parametrów modelu

$$D(L_p(\theta_p)) = -8\alpha sin(8\theta_p) \tag{37}$$

$$D(sat(i_p)) = -\epsilon\gamma e^{\epsilon i_p} \tag{38}$$

$$S(sat(i_p)) = \gamma i_p + \frac{\gamma}{\epsilon}(1 - e^{\epsilon i_p}) \tag{39}$$

$$\frac{di_p}{dt} = \frac{u_p - i_p R_p - 8\alpha\gamma\omega sin(8\theta_p)(1 - e^{\epsilon i_p})}{\beta - \alpha\gamma\epsilon(1 + cos(8\theta_p))e^{\epsilon i_p}} \tag{40}$$

$$T_p = 8\alpha\gamma sin(8\theta_p)(\frac{1}{\epsilon}(e^{\epsilon i_p} - 1) - i_p) \tag{41}$$

$$min_{P \in R^n} \sum_{i=1}^{l} \frac{1}{2}(\varphi(P;\tau_i) - d_i)^2, \tag{42}$$

where: φ is a nonlinear model equation (also called approximation function) of parameters set:

$$\boldsymbol{P} = [\alpha\ \beta\ \gamma\ \epsilon]^T\ , \tag{43}$$

i –sample number, d_i – measured quantity, τ_i is a vector of independent variables $\tau_i = [u_p, i_p, \theta_p, \omega]$ at sample number i. It may be said, that the goal expressed by (42) is to find set of parameters P values within a nonlinear model defined by φ so it agrees with measured values d_i as closely as possible. If defines an objective function f(x) based on (42), where x is a set of approximation function parameters P and variable θ_p : $x = [P; \tau_i]$.

There can be introduced parameter vector correction δ in n–iteration number as follows:

$$\boldsymbol{\delta}_n = \frac{-\boldsymbol{J}(\boldsymbol{x}_n)^T \boldsymbol{r}(\boldsymbol{x}_n)}{\boldsymbol{J}(\boldsymbol{x}_n)^T \boldsymbol{J}(\boldsymbol{x}_n) + \boldsymbol{Q}(\boldsymbol{x}_n)}, \tag{44}$$

$\boldsymbol{J}(\boldsymbol{x})^{l,k}$ is Jacobian of $f(\boldsymbol{x})$ in sizes: k — number of adjusted parameters (size of $\boldsymbol{P}$ vector), l — number of sampled reference values. Residual function values vector $\boldsymbol{r}$ is an approximation error in form:

$$r_i = \varphi_i - d_i, \tag{45}$$

and $\boldsymbol{r}$ symbol is a vector of: $\boldsymbol{r} = [r_1 \; r_2 \; ... \; r_{l-1} \; r_l]^T$.

New parameters value on each iteration are updated by using formula:

$$\boldsymbol{P}_n = \boldsymbol{P}_{n-1} + \boldsymbol{\delta}_n \boldsymbol{\eta}^T, \tag{46}$$

where: $\boldsymbol{\eta}$ is an vector of coefficients set for each model parameter in the range of $(0, 1)$.
Jacobian used in equation (44) elements are:

$$\boldsymbol{J}(\boldsymbol{x}) = \begin{bmatrix} \frac{\partial^2 f(x_1)}{\partial p_1} & \frac{\partial f(x_1)}{\partial p_2} & \dots & \frac{\partial f(x_1)}{\partial p_k} \\ \frac{\partial f(x_2)}{\partial p_1} & \frac{\partial f(x_2)}{\partial p_2} & \dots & \frac{\partial f(x_2)}{\partial p_k} \\ \vdots & \vdots & \ddots & \vdots \\ \frac{\partial f(x_l)}{\partial p_1} & \frac{\partial f(x_l)}{\partial p_k} & \dots & \frac{\partial f(x_l)}{\partial p_k} \end{bmatrix}. \tag{47}$$

$Q(x_n)$ is a part of the Hessian matrix that involves second derivatives of the residual function:

$$\boldsymbol{Q}(\boldsymbol{x}_n) = \sum_{i=1}^{m} r(x_i)\nabla^2 r(x_i) \tag{48}$$

$$\nabla^2 r(x_i) = \begin{bmatrix} \frac{\partial^2 f(x_i)}{\partial p_1 \partial p_1} & \frac{\partial^2 f(x_i)}{\partial p_1 \partial p_2} & \dots & \frac{\partial^2 f(x_i)}{\partial p_1 \partial p_k} \\ \frac{\partial^2 f(x_i)}{\partial p_2 \partial p_1} & \frac{\partial^2 f(x_i)}{\partial p_2 \partial p_2} & \dots & \frac{\partial^2 f(x_i)}{\partial p_2 \partial p_k} \\ \vdots & \vdots & \ddots & \vdots \\ \frac{\partial^2 f(x_i)}{\partial p_k \partial p_1} & \frac{\partial^2 f(x_i)}{\partial p_k \partial p_2} & \dots & \frac{\partial^2 f(x_i)}{\partial p_k \partial p_k} \end{bmatrix}. \tag{49}$$

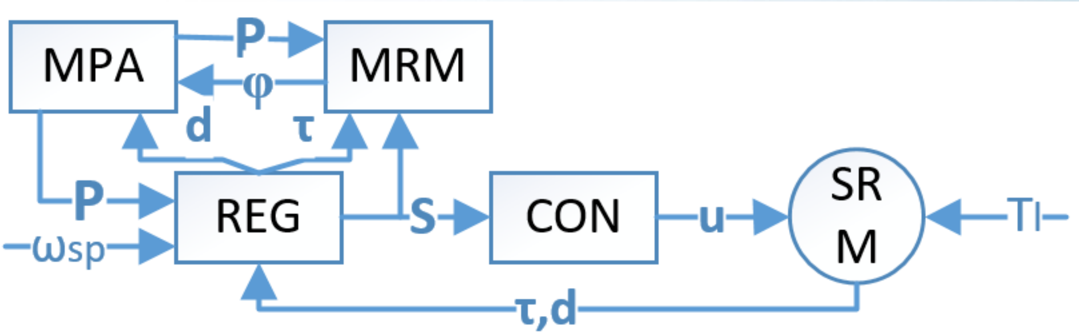

Rysunek 13: Structure of the SRM drive with model parameters adaptation system

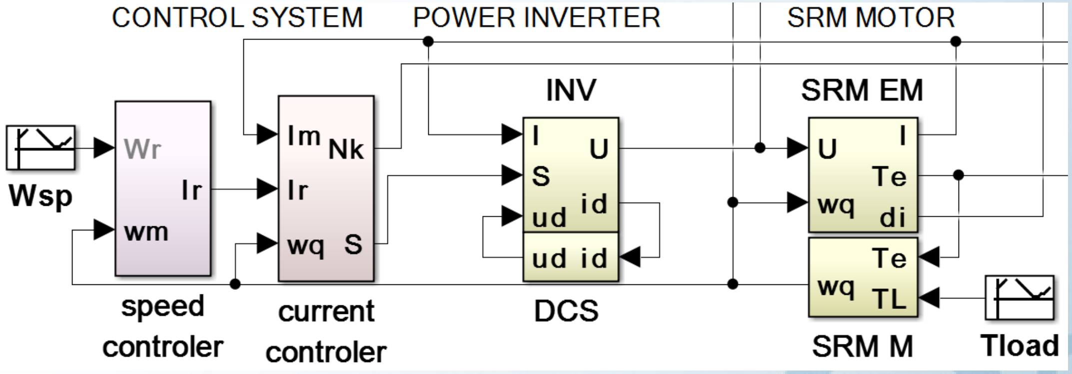

Rysunek 14: General control structure

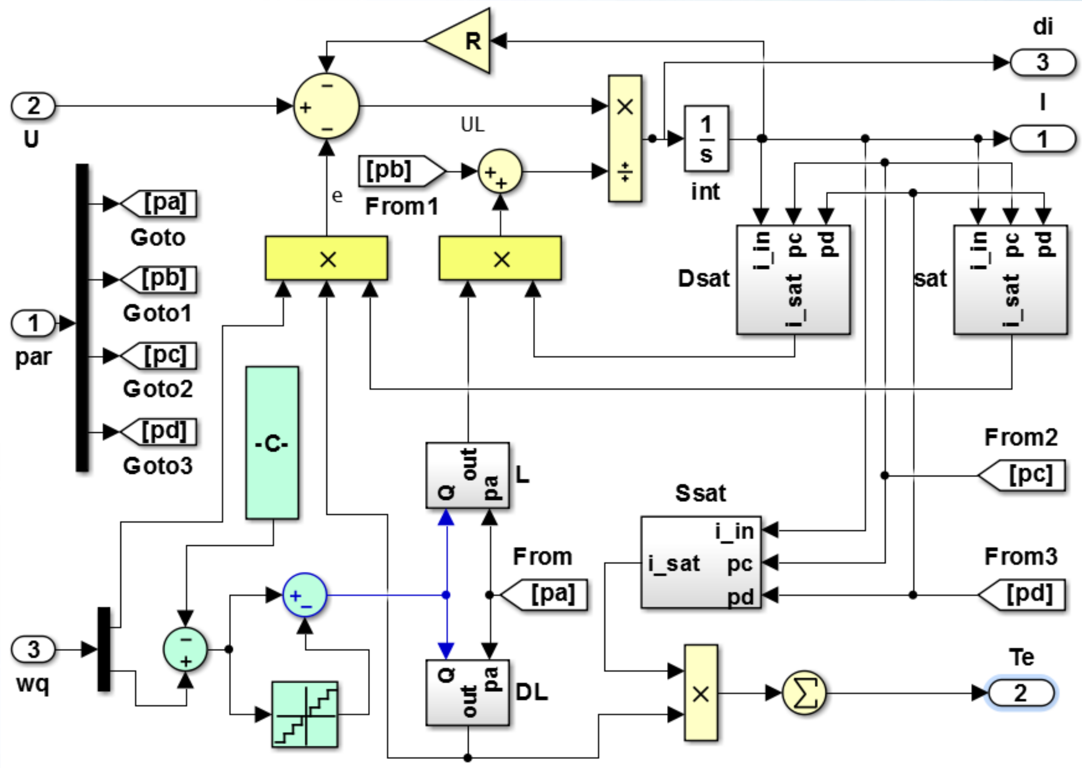

Rysunek 15: SRM reference model

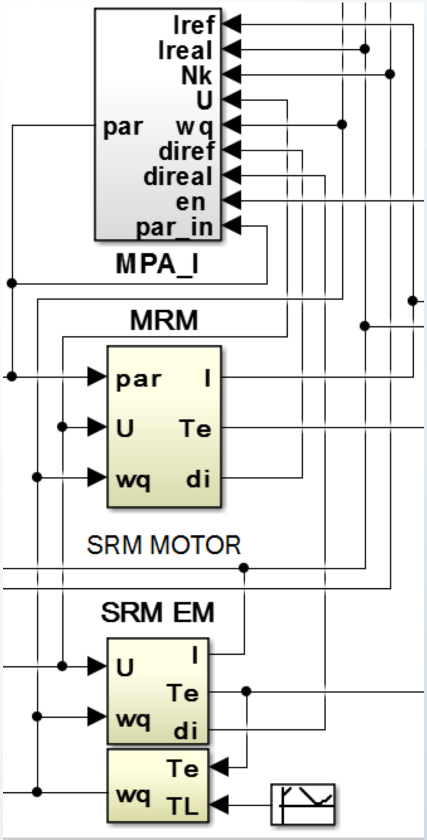

Rysunek 16: Implementation of MPA

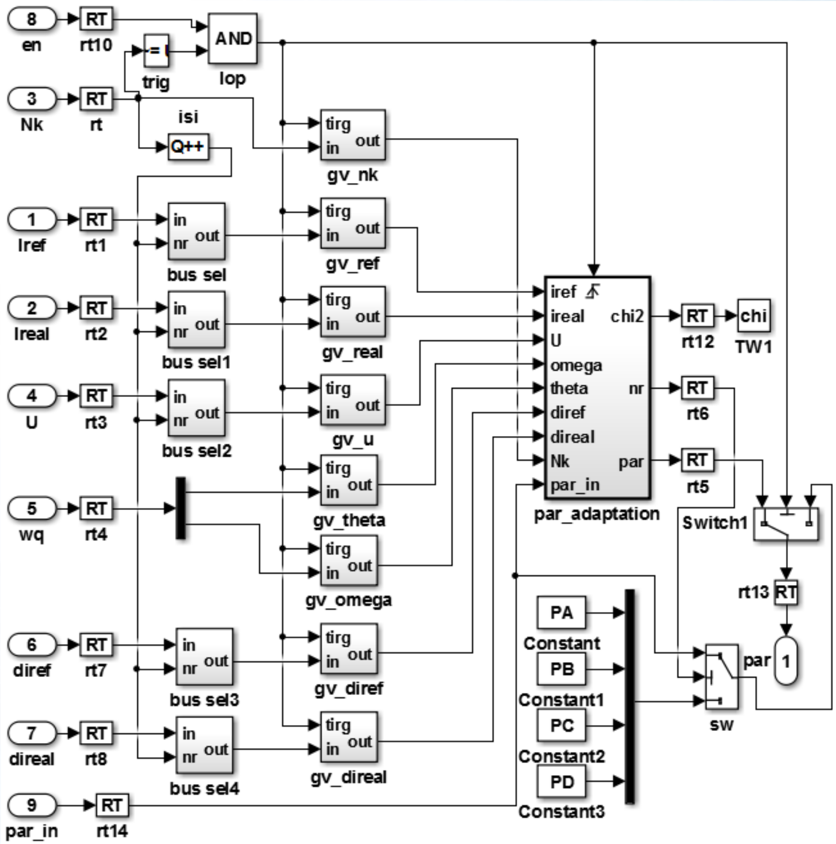

Rysunek 17: MPA block

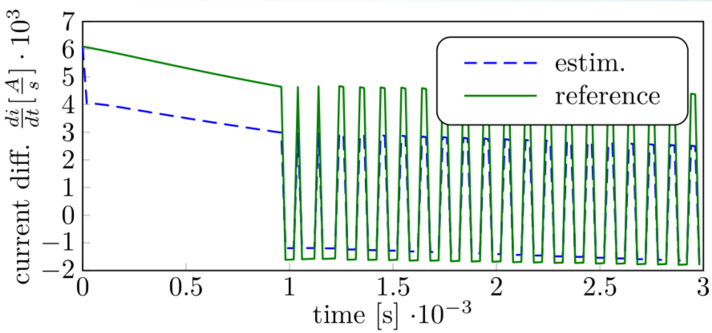

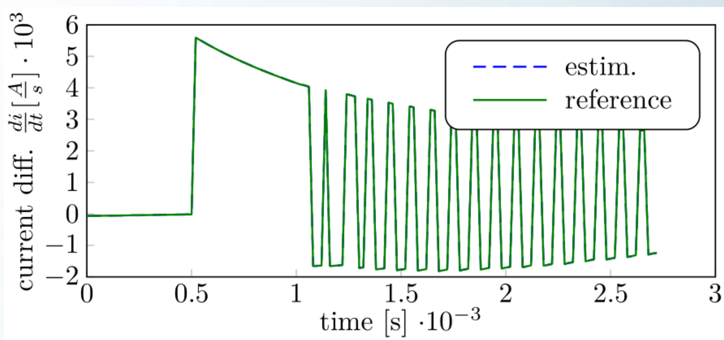

Rysunek 18: Phase current time derivatives vaweforms; at the fitting process start (top); at the end (bottom)

$$\chi_n^2 = \frac{\boldsymbol{r}(\boldsymbol{x}_n)^T \boldsymbol{r}(\boldsymbol{x}_n)}{\boldsymbol{\varphi}(\boldsymbol{x}_n)^T \boldsymbol{\varphi}(\boldsymbol{x}_n)} \tag{50}$$

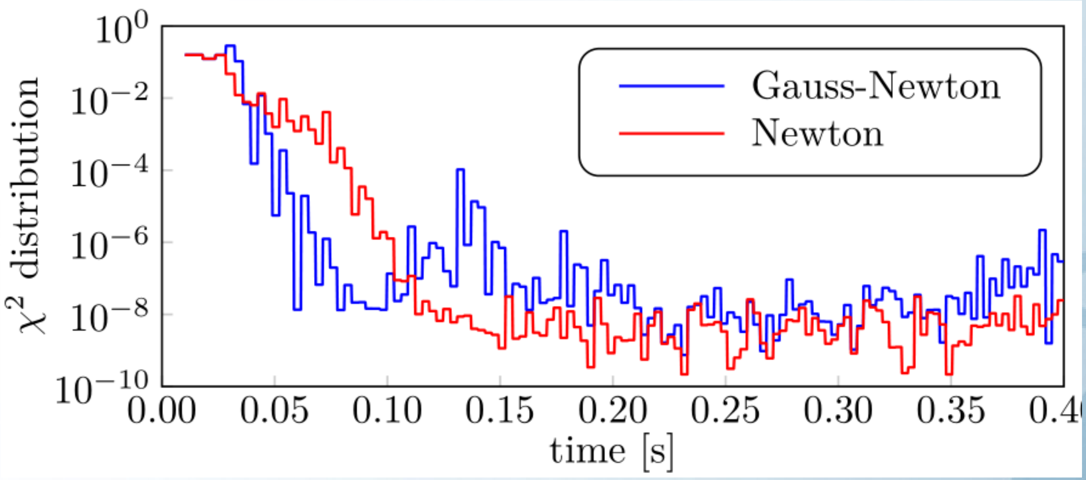

Rysunek 19: Chi2 (χ^2) indicator of parameters fitting process during time (with use of Gauss-Newton and Newton methods)

Wyznaczanie początkowego kąta obrotu wału

$$u_p = L_p \frac{di_p}{dt} \approx L_p \frac{\Delta i_p}{\Delta t} \quad (51)$$

$$L_p \approx u_p \frac{\Delta t}{\Delta i_p} \quad (52)$$

If define rotor global position θ_r for three phase $p = 1, 2, 3$ 12/8 poles switched reluctance motor, the relative phase position θ_p (to θ_r will be defined as follow – relation value $\frac{1}{12}\pi$ depends on motor geometry):

$$\theta_p = \theta_r - (p-1)\frac{\pi}{12}. \quad (53)$$

Considering phase inductance L_p as cosinusoidal rotor angle distribution dependence on parameters α – inductance amplitude and β – inductance constant offset (bias):

$$L_p(\theta_p, \alpha, \beta) = \alpha[cos(8\theta_p) + 1] + \beta, \tag{54}$$

inductance of all three motor phases are:

$$\begin{aligned} L_1(\theta_r, \alpha, \beta) =& \alpha\left[cos(8\theta_r) + 1\right] + \beta, \\ L_2(\theta_r, \alpha, \beta) =& \alpha\left[cos(8\theta_r - \frac{2}{3}\pi) + 1\right] + \beta, \\ L_3(\theta_r, \alpha, \beta) =& \alpha\left[cos(8\theta_r - \frac{4}{3}\pi) + 1\right] + \beta. \end{aligned} \tag{55}$$

$$
\begin{aligned}
L_1 - L_2 =& \alpha \left[cos(8\theta_r) - cos(8\theta_r - \frac{2}{3}\pi) \right], \\
L_1 - L_3 =& \alpha \left[cos(8\theta_r) - cos(8\theta_r - \frac{4}{3}\pi) \right],
\end{aligned} \tag{56}
$$

using general trigonometric rule:

$$
cos(x) - cos(y) = -2sin((x+y)/2)sin((x-y)/2) \tag{57}
$$

equations 56 becomes:

$$
\begin{aligned}
L_1 - L_2 =& -2\alpha sin(8\theta_r - \frac{1}{3}\pi) sin(\frac{1}{3}\pi), \\
L_1 - L_3 =& -2\alpha sin(8\theta_r - \frac{2}{3}\pi) sin(\frac{2}{3}\pi).
\end{aligned} \tag{58}
$$

When divide both expressions from 58:

$$\overbrace{\frac{L_1 - L_2}{L_1 - L_3}}^{a} = \frac{sin(8\theta_r - \frac{1}{3}\pi)}{sin(8\theta_r - \frac{2}{3}\pi)} \overbrace{\frac{sin(\frac{1}{3}\pi)}{sin(\frac{2}{3}\pi)}}^{b} \tag{59}$$

and use another trigonometric expression:

$$sin(x - y) = sin(x)cos(y) - cos(x)sin(y) \tag{60}$$

an equation may be formulated:

$$\frac{a}{b} = \frac{sin(8\theta_r)cos(1/3\pi) - cos(8\theta_r)sin(1/3\pi)}{sin(8\theta_r)cos(2/3\pi) - cos(8\theta_r)sin(2/3\pi)}. \tag{61}$$

Introducing shorter notification of sine function as s and cosine c respectively, $8\theta_r$ as just θ the expression 61 may be written:

$$a\left[s(\theta)c(\frac{2}{3}\pi) - c(\theta)s(\frac{2}{3}\pi)\right] = b\left[s(\theta)c(\frac{1}{3}\pi) - c(\theta)s(\frac{1}{3}\pi)\right] \quad (62)$$

After ordering with respect to variable θ:

$$s(\theta)\overbrace{\left[ac(\frac{2}{3}\pi) - bc(\frac{1}{3}\pi)\right]}^{m} + c(\theta)\overbrace{\left[bs(\frac{1}{3}\pi) - as(\frac{2}{3}\pi)\right]}^{n} = 0. \quad (63)$$

Equation (63) can be rearranged to the form:

$$\frac{s(\theta)}{c(\theta)} = -\frac{n}{m}. \quad (64)$$

While $s(\theta)/c(\theta) = tg(\theta)$:

$$tg(8\theta_r) = -\frac{n}{m} \tag{65}$$

and finally:

$$\theta_r = \frac{1}{8} atan2(-n, m). \tag{66}$$

$$\alpha = \frac{L_1 - L_2}{cos(8\theta_r) - cos(8\theta_r - \frac{2}{3}\pi)} \tag{67}$$

$$\beta = L_2 - \alpha \left[cos(8\theta_r - \frac{2}{3}\pi) + 1 \right] \tag{68}$$

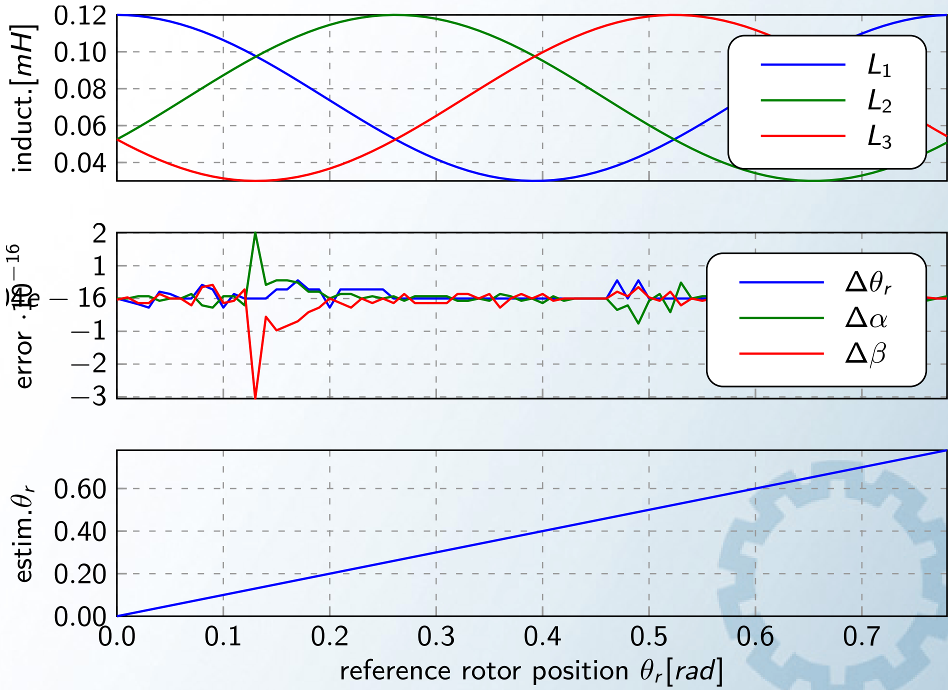

Rysunek 20: Results of the phase inductance angular distribution model parameter estimation based on the artificially generated functions $L_p, p = 1, 2, 3$ waveforms

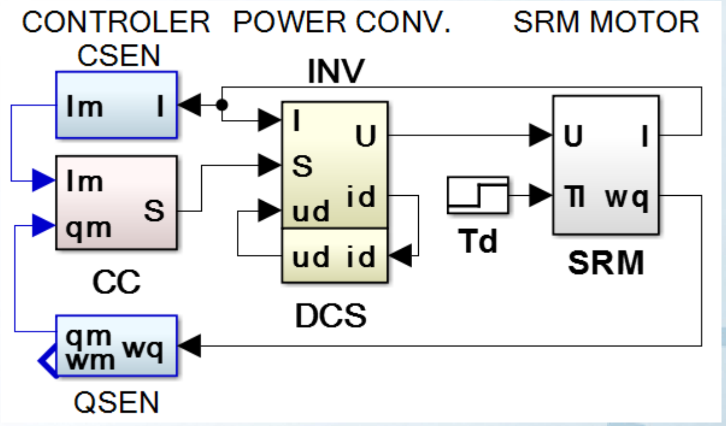

Rysunek 21: General simulation system structure

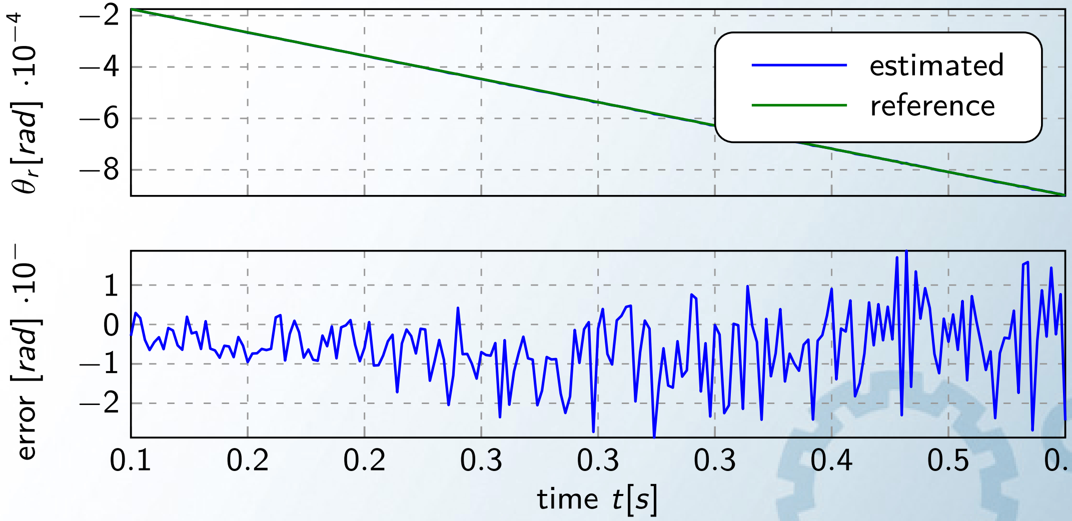

Rysunek 22: Waveforms of the on-line motor rotor angle estimation process - absolute values (top), estimation error (bottom)

Optymalizacja sterowania

Funkcja $i_p(T_p)$

$$T_p(\theta_p, i_p) = [-8\alpha\gamma sin(8\theta_p)] \left[i_p - \frac{1}{\epsilon}\left(e^{\epsilon i_p} - 1\right)\right] \tag{69}$$

$$T_p(\theta_p, i_p) = T_{p\theta} T_{pi} \tag{70}$$

$$T_p(i_p)_{T_{p\theta}=K} = K T_{pi} \tag{71}$$

$$i_p - \frac{1}{\epsilon} e^{\epsilon i_p} = \frac{T_p}{K} - \frac{1}{\epsilon} \tag{72}$$

$$i_p = -\frac{1}{\epsilon}\left[\frac{K - T_p\epsilon}{K} + W\left(-e^{-\frac{K-T_p\epsilon}{K}}\right)\right] \tag{73}$$

Operator Lamberta W

$$z = f^{-1}(ze^z) = W(ze^z) \tag{74}$$

$$z = f^{-1}(xe^x) = W(xe^x) \tag{75}$$

The Lambert W relation cannot be expressed in terms of elementary functions. It can be used to solve various equations involving exponentials (e.g. the maxima of the Planck, Bose–Einstein, and Fermi–Dirac distributions).

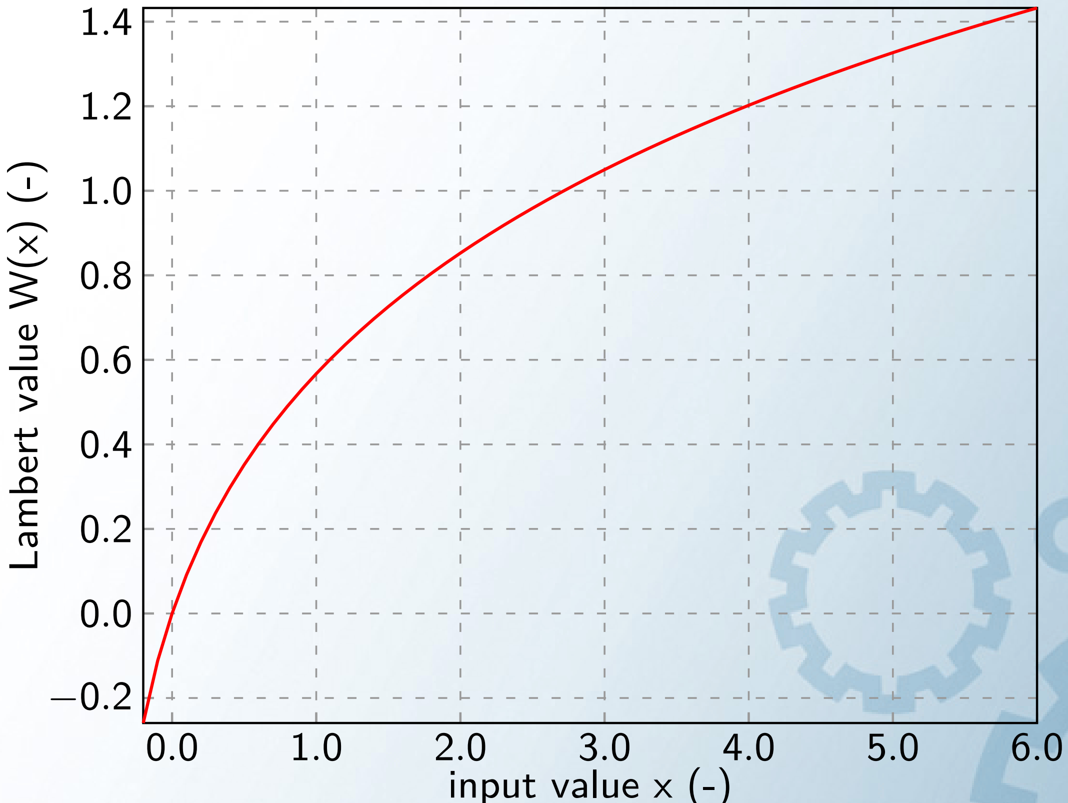

Rysunek 23: Lambert f=W(x) plot

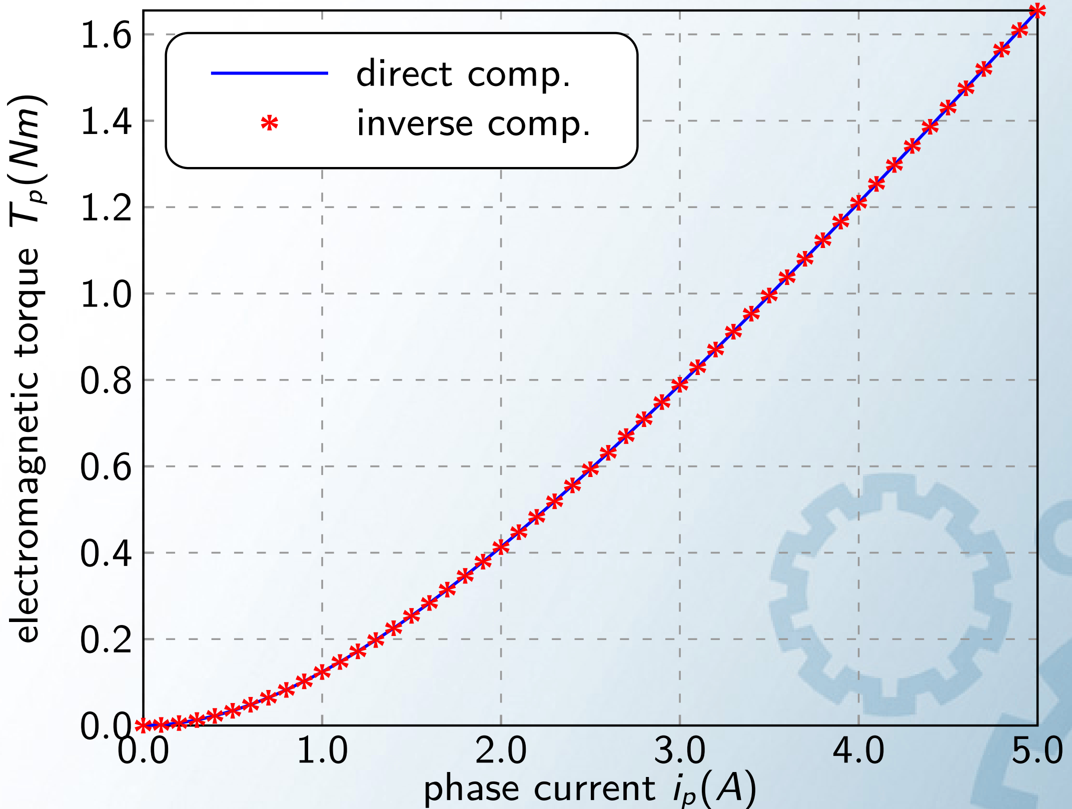

Rysunek 24: Lambert W solving test example by $T_p = f(i_p)$ inversing

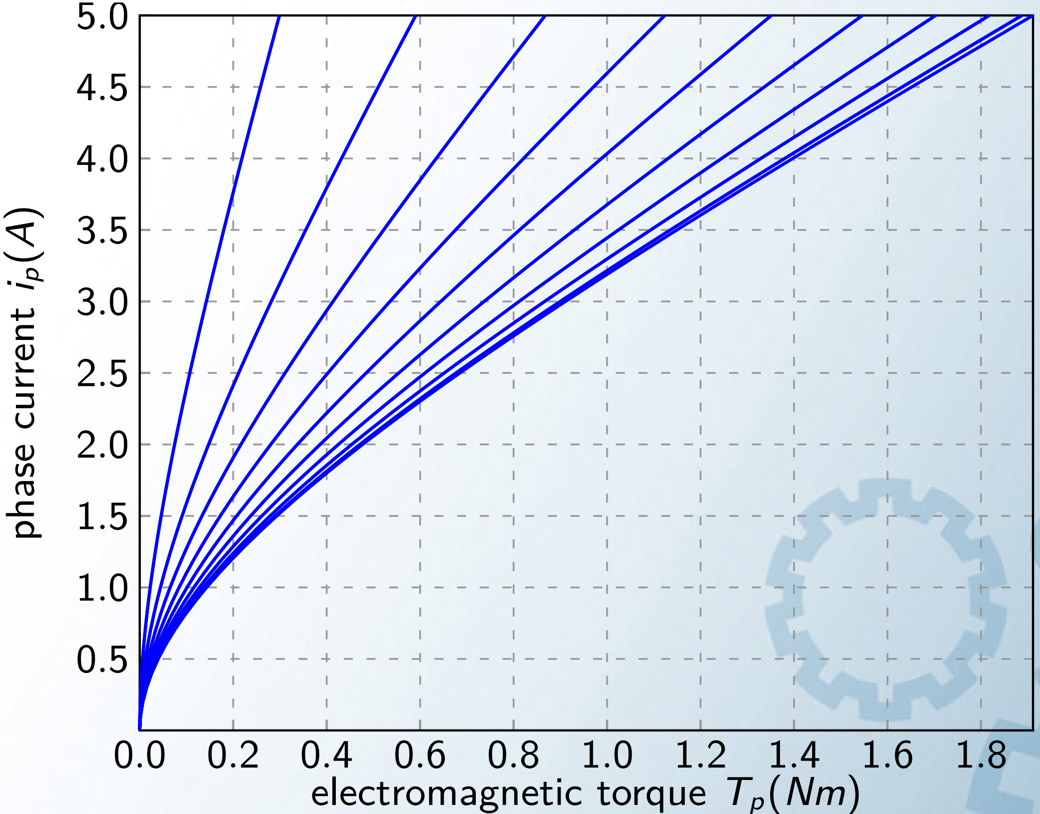

Rysunek 25: Function of $i_p = f(T_p)$ at different θ_p values (-π;π)

Optymalizacja kątów komutacji

Przypadek wyidealizowany

$$T_p(\theta_p, i_p) = [-8\alpha\gamma sin(8\theta_p)]\left[i_p - \frac{1}{\epsilon}\left(e^{\epsilon i_p} - 1\right)\right] \tag{76}$$

$$T_p(\theta_p, i_p) = T_{p\theta} T_{pi} \tag{77}$$

Przy braku opóźnień w torze sterowania oraz pomijając fazy narastania oraz wygaszania prądów poszczególnych pasm zagadnienie sprowadza się do określenia:

$$max(\theta_p)\ T_p(\theta_p, i_p = i_{sp}) \tag{78}$$

$$f(x) = \int_{x=\theta_{on}}^{\theta_{on}+2/3\pi} sin(x)dx \tag{79}$$

$$f(x) = cos(\theta_{on} + 2/3\pi) - cos(\theta_{on}) \quad (80)$$

$$f'(x) = -sin(\theta_{on} + 2/3\pi) + sin(\theta_{on}) \quad (81)$$

$$f'(x) = -\left[sin(\theta_{on})cos(2/3\pi) + sin(2/3\pi)cos(\theta_{on})\right] + sin(\theta_{on}) \quad (82)$$

$$f'(x) = sin(\theta_{on})\underbrace{(1 - cos(2/3\pi))}_{A} - cos(\theta_{on})\underbrace{sin(2/3\pi)}_{B} = 0 \quad (83)$$

$$Asin(\theta_{on}) = Bcos(\theta_{on}) \quad (84)$$

$$\theta_{on} = atan2(B, A) = 0.524(rad) \quad (85)$$

$$\theta_{on} = atan2(-B, -A) = -\pi/2 - \pi/3 = -2.618(rad) \quad (86)$$

rozwiązanie (85) znajduje minimum, maksimum jest w 3-ciej ćwiartce (x<0, y<0) – (86).

W rozwiązaniu ogólnym kryterium maksimum uzyskiwanego momentu elektromagnetycznego należy uwzględnić opóźnienia w torze sterowania, czas oraz samą funkcję narastania/wygaszania prądu uzwojenia pasma silnika. W takim przypadku znalezienie optimum uzyskiwanego momentu elektromagnetycznego sprowadza się do poszukania maksimum dla całki z funkcji sumy trzech składowych momentu elektromagnetycznego (faza narastania prądu, faza utrzymywania wartości stałej, faza demagnetyzacji):

$$T_p = T_{pr} + T_{pc} + T_{pf} \tag{87}$$

W rozwiązaniu zagadnienia minimalizacji tętnień momentu należy przejść z domeny prądów fazowych na domenę momentu elektromagnetycznego. W zakresie sterowania poza nasyceniami można kształtować przebieg prądu z wykorzystaniem funkcji odwrotnej celem utrzymywania stałego momentu. W zakresie nasyceń są trzy możliwości:

- wybór kąta załączenia tak, aby czasy narastania i

Blok detekcji uszkodzeń

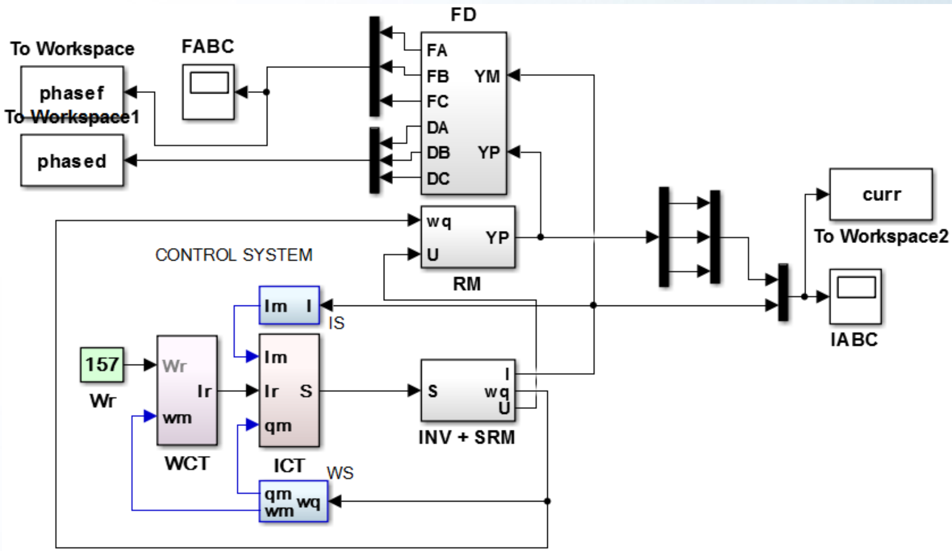
FD
To Workspace
FABC
phasef
To Workspace1
phased
FA
FB
FC
DA
DB
DC
YM
YP
wq
U
YP
RM
CONTROL SYSTEM
curr
To Workspace2
IABC
Im
I
IS
157
Wr
Wr
Ir
wm
WCT
Im
Ir
S
qm
ICT
S
I
wq
U
INV + SRM
WS
qm
wm
wq

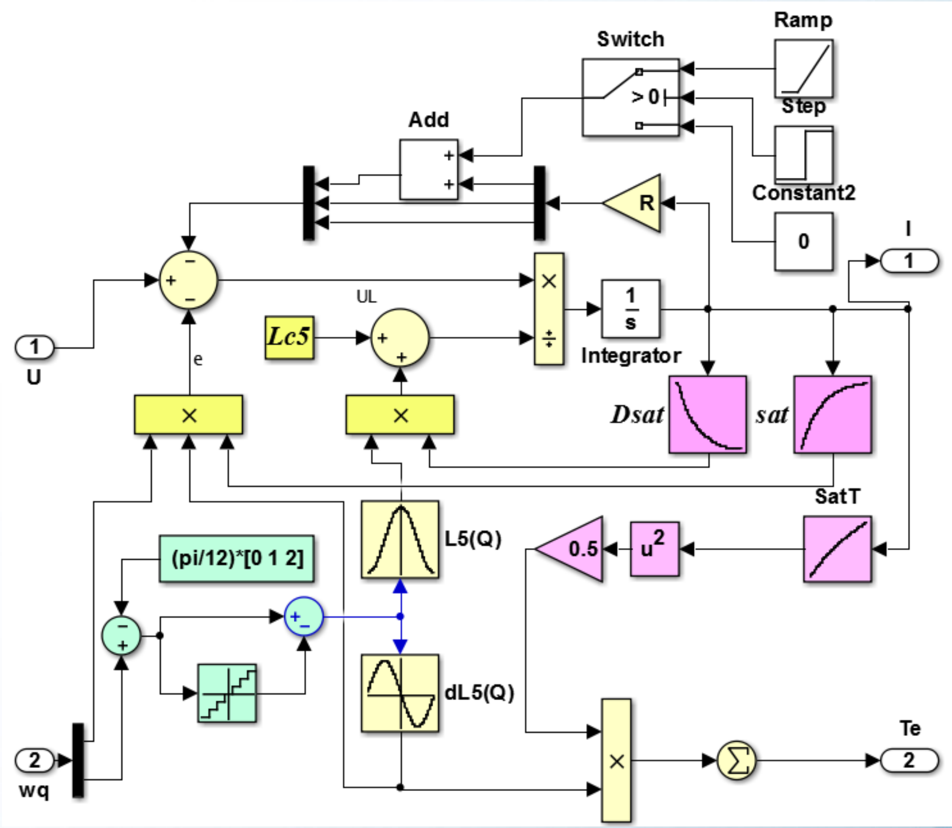
Ramp
Switch
> 0
Step
Add
Constant2
R
0
I
1
UL
1
s
Integrator
Lc5
1
U
e
Dsat
sat
SatT
L5(Q)
(pi/12)*[0 1 2]
0.5
u2
dL5(Q)
Te
2
2
wq

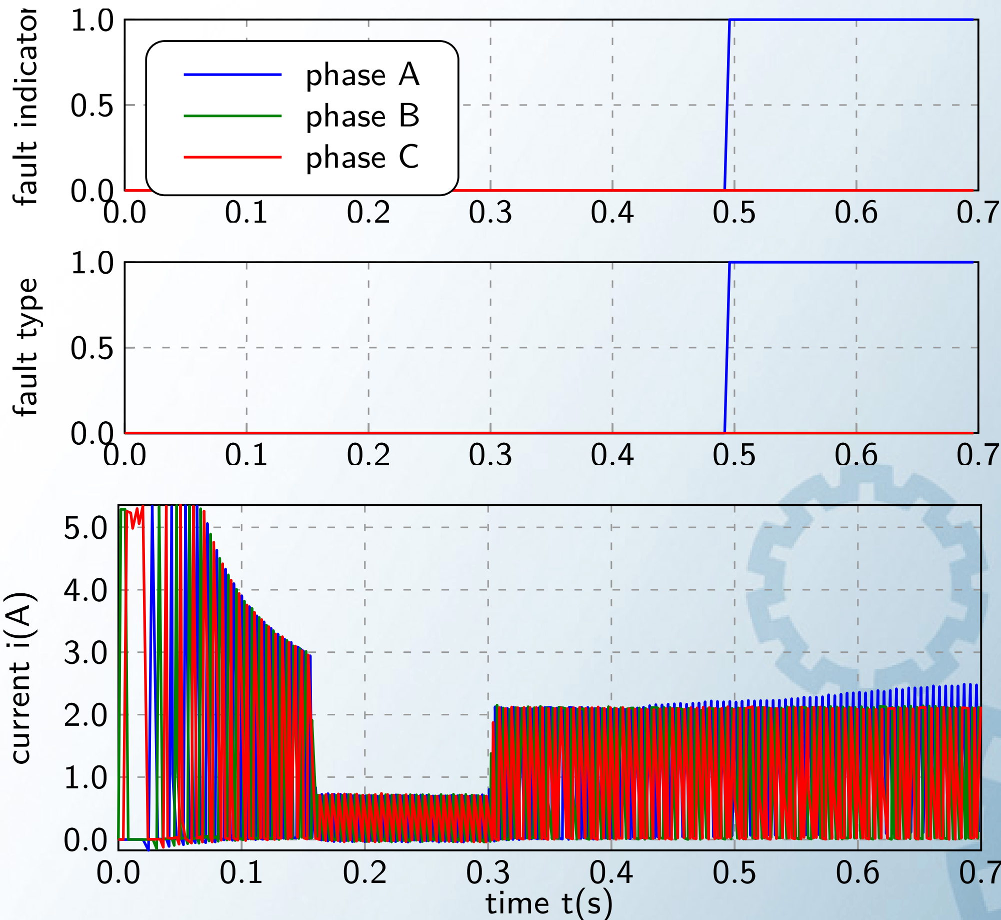

fault indicator
fault type
current i(A)
time t(s)
phase A
phase B
phase C
1.0
0.5
0.0
5.0
4.0
3.0
2.0
0.1
0.2
0.3
0.4
0.6
0.7

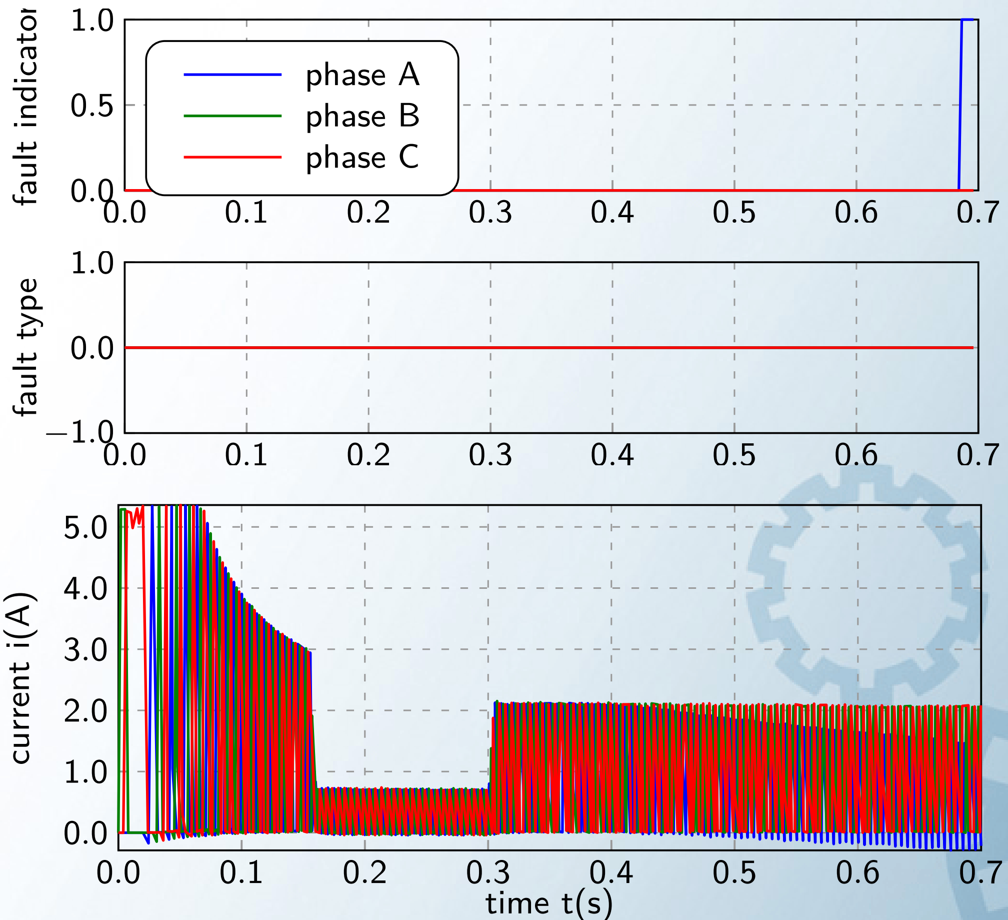
fault indicator
1.0
0.5
0.0
phase A
phase B
phase C
0.0 0.1 0.2 0.3 0.4 0.5 0.6 0.7
fault type
1.0
0.0
−1.0
0.0 0.1 0.2 0.3 0.4 0.5 0.6 0.7
current i(A)
5.0
4.0
3.0
2.0
1.0
0.0
0.0 0.1 0.2 0.3 0.4 0.5 0.6 0.7
time t(s)

Podsumowanie

- przedstawiono zasadę działania silnika SRM
- wyprowadzono szczegółowy, parametryczny model silnika
- omówiono procedurę adaptacji parametrów w systemie on-line
- dokonano wykładni analitycznej: koncepcji wyznaczania położenia początkowego wału, funkcji odwrotnej momentu, podejścia optymalizacji kątów wysterowania
- omówiono zmodyfikowaną wersję bloku detekcji uszkodzeń z przykładem działania

Do realizacji

- bezczujnikowy pomiar położenia/prędkości wału
- opracowanie estymatora momentu obciążenia
- opracowanie bloku FTC na bazie przedstawionych zależności analitycznych
- dokończenie konstrukcji stanowiska eksperymentalnego
- eksperymentalna weryfikacja algorytmów